



1 **Concentration, sources and light absorption**  
2 **characteristics of dissolved organic carbon on a typical**  
3 **glacier, the northeastern Tibetan Plateau**

4 **F. Yan<sup>1,4,5</sup>, S. Kang<sup>1,3\*</sup>, C. Li<sup>2,3\*</sup>, Y. Zhang<sup>1</sup>, X. Qin<sup>1</sup>, Y. Li<sup>2,4</sup>, X. Zhang<sup>1,4</sup>, Z. Hu<sup>1,4</sup>, P. Chen<sup>2</sup>, X. Li<sup>1</sup>,**  
5 **B. Qu<sup>5</sup>, M. Sillanpää<sup>5,6</sup>**

6 <sup>1</sup>Qilian Station for Glaciology and Ecological Environment, State Key Laboratory of Cryospheric  
7 Sciences, Cold and Arid Regions Environmental and Engineering Research Institute, Chinese Academy  
8 of Sciences, Lanzhou 730000, China

9 <sup>2</sup>Key Laboratory of Tibetan Environment Changes and Land Surface Processes, Institute of Tibetan  
10 Plateau Research, Chinese Academy of Sciences, Beijing 100101, China

11 <sup>3</sup>CAS Center for Excellence in Tibetan Plateau Earth Sciences, Chinese Academy of Sciences, Beijing  
12 100101, China

13 <sup>4</sup>University of Chinese Academy of Sciences, Beijing 100049, China

14 <sup>5</sup>Laboratory of Green Chemistry, Lappeenranta University of Technology, Sammonkatu 12, FIN-50130  
15 Mikkeli, Finland

16 <sup>6</sup>Department of Civil and Environmental Engineering, Florida International University, Miami, FL 33174,  
17 USA

18 *Correspondence to:* C. Li ([lichao.li@itpcas.ac.cn](mailto:lichao.li@itpcas.ac.cn))

19 **Abstract.** Light-absorbing dissolved organic carbon (DOC) constitutes a major part of the organic carbon  
20 in the glacierized region. It has important influences on the carbon cycle and radiative forcing of glaciers.  
21 However, currently, few data are available in the glacierized region of the Tibetan Plateau (TP). In this  
22 study, DOC characteristics of a typical glacier (Laohugou glacier No. 12 (LHG glacier)) in the  
23 Northeastern TP were investigated. Generally, DOC concentrations on LHG glacier were comparable to  
24 other glacierized regions around the world. The average DOC concentrations in snowpits, surface snow,  
25 surface ice (superimposed ice) and proglacial streamwater were  $332.4 \pm 132.3 \mu\text{g L}^{-1}$ ,  $229.3 \pm 104.4 \mu\text{g L}^{-1}$



26 <sup>1</sup>,  $425.8 \pm 269.9 \mu\text{g L}^{-1}$ , and  $237.5 \pm 95.6 \mu\text{g L}^{-1}$ , respectively. It was estimated that the annual DOC flux  
27 released from this glacier was  $6,949.4 \text{ kg C yr}^{-1}$ , of which 43.2% DOC was bioavailable and could be  
28 decomposed into  $\text{CO}_2$  within 28 days of its release. The mass absorption cross section (MAC) of DOC  
29 at 365 nm was  $1.4 \pm 0.4 \text{ m}^2 \text{ g}^{-1}$  in snow and  $1.3 \pm 0.7 \text{ m}^2 \text{ g}^{-1}$  in ice, similar to those of dust transported from  
30 adjacent deserts. Based on this finding and the significant relationship between DOC and  $\text{Ca}^{2+}$ , it was  
31 proven that the main source of DOC of this glacier was mineral dust. The radiative forcing of DOC  
32 relative to black carbon (BC) was calculated to be  $9.5 \pm 8.4 \%$  in snow and  $0.1 \pm 0.1 \%$  in ice, respectively,  
33 implying the necessity of accounting for DOC in future radiative forcing investigations in the glacierized  
34 region on the TP, especially when these areas are covered by fresh snow.

35 **Key words:** dissolved organic carbon, concentration, light absorption, LHG glacier, the Tibetan Plateau  
36



## 37 **1 Introduction**

38 Ice sheets and mountain glaciers cover 11% of the land surface of the Earth and store approximately  
39 6 Pg (1 Pg=10<sup>15</sup> g) of organic carbon, the majority of which (77%) is in the form of dissolved organic  
40 carbon (DOC) (Hood et al., 2015). The annual global DOC release through glacial runoff is  
41 approximately 1.04±0.18 Tg C (1 Tg=10<sup>12</sup> g) (Hood et al., 2015). Therefore, glaciers not only play  
42 important role in the hydrological cycle by contributing to sea-level rise (Rignot et al., 2003; Jacob et al.,  
43 2012), but also potentially influence the global carbon cycle (Anesio and Laybourn-Parry, 2012; Hood  
44 et al., 2015) in the context of accelerated glacial ice loss rates. In addition, a large portion of glacier-  
45 released DOC has proven to be highly bioavailable, influencing the balance of downstream ecosystems  
46 (Hood et al., 2009; Singer et al., 2012).

47 Although DOC storage in ice sheets is much larger than that of mountain glaciers, the annual  
48 mountain glacier-derived DOC dominates the global DOC release (Hood et al., 2015). Currently, many  
49 studies on the concentration, age, composition, storage and release of DOC have been conducted around  
50 the world (Stubbins et al., 2012; Bhatia et al., 2013; Lawson et al., 2014 ; Hood et al., 2015). The sources  
51 of glacier-derived DOC were found to be diverse (Bhatia et al., 2010; Stubbins et al., 2012; Singer et al.,  
52 2012), with large variations in concentrations and ages (Singer et al., 2012; Hood et al., 2015). For  
53 example, a study on the Greenland ice sheet showed that the concentration of exported DOC exhibited  
54 slight temporal variations during the melting period, with subtly higher values in early May than late  
55 May and July (Bhatia et al., 2013). Additionally, concentration of total organic carbon in snow across the  
56 East Antarctic ice sheets exhibited remarkable spatial variations due to the marine source of organic  
57 carbon (Antony et al., 2011). Studies on both radiocarbon isotopic compositions and biodegradable DOC  
58 (BDOC) have proposed that ancient organic carbon from glaciers was much easier for microbes to utilize  
59 in glacier-fed rivers and oceans, implying that large amounts of these DOC will return to the atmosphere  
60 quickly as CO<sub>2</sub> and participate in the global carbon cycle, thereby producing a positive feedback in the  
61 global warming process (Hood et al., 2009; Singer et al., 2012). In addition to black carbon (BC), another  
62 DOC fraction known as water-soluble brown carbon (WS-BrC) has also been considered a warming  
63 component in the climate system (Andreae and Gelencs ́r, 2006; Chen and Bond, 2010). This type of  
64 DOC exhibits strong light-absorbing properties in the ultraviolet wavelengths (Andreae and Gelencs ́r,  
65 2006; Chen and Bond, 2010). The relative radiative forcing caused by water-soluble organic carbon  
66 (WSOC, the same as DOC) relative to BC in aerosols was estimated to account for 2-10% and



67 approximately 1% in a typical pollution area of North China (Kirillova et al., 2013) and a remote island  
68 in the Indian Ocean (Bosch et al., 2014), respectively. Unfortunately, so far, few direct evaluations have  
69 been conducted in the glacierized region around the world, including the Tibetan Plateau (TP), where  
70 DOC accounts for a large part of the carbonaceous matter (Legrand et al., 2013; May et al., 2013) and  
71 potentially contributes to radiative forcing in the glacierized region.

72 The TP has the largest number of glaciers at moderate elevations. Most of the glaciers on the TP are  
73 experiencing intensive retreat because of increases in temperature (Kang et al., 2010; Yao et al., 2012;  
74 Kang et al., 2015) and anthropogenic carbonaceous particle deposition (Xu et al., 2009; Qu et al., 2014;  
75 Kaspari et al., 2014). However, to date, no study has quantitatively evaluated the light absorption  
76 characteristics of DOC in the glacierized region on the TP, despite some investigations of concentrations  
77 and sources (Spencer et al., 2014; Yan et al., 2015). The primary results of these studies have showed  
78 that DOC concentrations in snowpits in the northeastern TP were higher than those in the southern TP  
79 (Yan et al., 2015). In addition, a large fraction of the ancient DOC in the glacier in the southern TP has  
80 high bioavailability characteristics (Spencer et al., 2014). However, knowledge of DOC in TP glaciers  
81 remains lacking due to the large area and diverse environments of the TP and the relatively limited  
82 samples and studies. Therefore, numerous snow, ice and proglacial streamwater samples (n=310) (Table  
83 S1, Fig. 1) were collected from a typical glacier in the northeastern TP (Laohugou glacier No. 12 (LHG  
84 glacier)) based on the preliminary research of snowpit samples (Yan et al., 2015). The concentrations of  
85 DOC and major ions ( $\text{Ca}^{2+}$ ,  $\text{Mg}^{2+}$ ,  $\text{Na}^+$ ,  $\text{K}^+$ ,  $\text{NH}_4^+$ ,  $\text{Cl}^-$ ,  $\text{NO}_3^-$  and  $\text{SO}_4^{2-}$ ) and DOC light absorbance were  
86 measured to comprehensively investigate the sources, light absorption characteristics and carbon  
87 dynamics in this glacierized region to provide a basis for the study of DOC across the TP and other regions  
88 in the future.

## 89 2 Methodology

### 90 2.1 Study area and sampling site

91 LHG glacier is the largest mountain glacier (9.85 km, 20.4 km<sup>2</sup>) in the Qilian Mountains located on  
92 the northeastern edge of the TP (39°05'-40'N, 96°07'-97°04'E 4260-5481 m) (Du et al., 2008; Dong et al.,  
93 2014a). This glacier is surrounded by large arid and semi-arid regions (sandy deserts and the Gobi desert)  
94 (Fig. 1). The area of the glacier covers approximately 53.6% of the entire LHG glacier basin (Du et al.,  
95 2008; Li et al., 2012).

96 The LHG glacier features typical continental and arid climate characteristics (Li et al., 2012; Zhang



97 et al., 2012b). Precipitation occurs mainly from May to September, accounting for over 70% of the total  
98 annual precipitation (Zhang et al., 2012b). The monthly mean air temperatures in the ablation zone of  
99 the glacier range from -18.4 °C in December to 3.4 °C in July (Li et al., 2012). Like other glaciers on the  
100 TP, LHG glacier has been experiencing significant thinning and shrinkage at an accelerated rate since the  
101 mid-1990s (Du et al., 2008; Zhang et al., 2012b).

## 102 **2.2 Sample collection**

103 Two snowpits were dug in 2014 and 2015 in the accumulation zone of LHG glacier. In total, 15 and  
104 23 snow samples were collected in 2014 and 2015, respectively, at a vertical resolution of 5 cm for each  
105 snowpit. Moreover, 71 snow/ice samples were collected along the eastern tributary at an approximate  
106 elevation interval of 50 or 100 m from the terminus to the accumulation zone, and 201 proglacial  
107 streamwater samples were collected at the gauge station during the melting period (Fig. 1, Table S1). The  
108 concentrations of glacier DOC have been observed to be very low and prone to contamination, causing  
109 an overestimation of DOC concentration (Legrand et al., 2013). Therefore, during the whole sampling  
110 procedure, samples were collected according to the “Clean hands-Dirty Hands” principle to prevent any  
111 contamination (Fitzgerald, 1999). Meanwhile, at least one blank was made for every sampling process  
112 to confirm that the contamination was low (Table S2). Moreover, another batch of samples were also  
113 collected for BC concentration measurement following the protocol discussed in detail in our earlier  
114 work (Qu et al., 2014) and these results will be presented in another article.

115 All the collected samples were stored in 125 mL pre-cleaned polycarbonate bottles, kept frozen and  
116 in the dark in the field, during transportation and in the laboratory until analysis. In addition, two sand  
117 samples from the desert and four dust samples from Dunhuang (39°53'–41°35'N, 92°13'–93°30'E) – a  
118 potential source region of the dust deposited on LHG glacier – were collected to compare the light  
119 absorption characteristic of dust-sourced DOC to those of the snowpit and ice samples.

## 120 **2.3 Laboratory analyses**

### 121 **2.3.1 Concentration measurements of DOC and major ions**

122 DOC concentrations were determined using a TOC-5000A analyzer (Shimadzu Corp, Kyoto, Japan)  
123 after the collected samples were filtered through a PTFE membrane filter with 0.45 µm pore size  
124 (Macherey–Nagel) (Yan et al., 2015). The detection limit of the analyzer was 15 µg L<sup>-1</sup>, and the average  
125 DOC concentration of the blanks was 31.9±7.4 µg L<sup>-1</sup>, demonstrating that contamination can be ignored



126 during the pre-treatment and analysis processing of these samples (Table S2). The major cations ( $\text{Ca}^{2+}$ ,  
 127  $\text{Mg}^{2+}$ ,  $\text{Na}^+$ ,  $\text{K}^+$  and  $\text{NH}_4^+$ ) and major anions ( $\text{Cl}^-$ ,  $\text{NO}_3^-$  and  $\text{SO}_4^{2-}$ ) were measured using a Dionex-6000 Ion  
 128 Chromatograph and a Dionex-3000 Ion Chromatograph (Dionex, USA), respectively. The detection limit  
 129 was  $1 \mu\text{g L}^{-1}$ , and the standard deviation was less than 5 % (Li et al., 2007; Li et al., 2010). The average  
 130 ion concentrations of the blank were very low and could be ignored ( $\text{Na}^+$ ,  $\text{K}^+$ ,  $\text{Mg}^{2+}$ ,  $\text{F}^+$ ,  $\text{SO}_4^{2-}$ ,  $\text{Cl}^-$ ,  $\text{NO}_3^-$  <  
 131  $1 \mu\text{g L}^{-1}$ ;  $\text{NH}_4^+=1.4 \mu\text{g L}^{-1}$ ;  $\text{Ca}^{2+}=1.2 \mu\text{g L}^{-1}$ ).

### 132 2.3.2 Light absorption measurements

133 The light absorption spectra of DOC was measured using an ultraviolet-visible absorption  
 134 spectrophotometer (SpectraMax M5, USA), scanning wavelengths from 200-800 nm at a precision of 5  
 135 nm. The mass absorption cross section (MAC) was calculated based on the Lambert-Beer Law (Bosch  
 136 et al., 2014; Kirillova et al., 2014a; Kirillova et al., 2014b):

$$137 \quad \text{MAC}_{\text{DOC}} = \frac{-\ln\left(\frac{I}{I_0}\right)}{C \cdot L} = \frac{A}{C \cdot L} \times \ln(10) \quad (1)$$

138 where  $I_0$  and  $I$  are the light intensities of the transmitted light and incident light, respectively,  $A$  is the  
 139 absorbance derived directly from the spectrophotometer,  $C$  is the concentration of DOC, and  $L$  is the  
 140 absorbing path length (1 cm).

141 In order to investigate the wavelength dependence of DOC light absorption characteristics, the  
 142 Absorption Ångström Exponent (AAE) was fitted by the following equation (Kirillova et al.,  
 143 2014a; Kirillova et al., 2014b):

$$144 \quad \frac{A(\lambda_1)}{A(\lambda_2)} = \left(\frac{\lambda_2}{\lambda_1}\right)^{\text{AAE}} \quad (2)$$

145 AAE values were fitted from the wavelength of 330 to 400 nm, within this wavelength range, light  
 146 absorption by other inorganic compounds can be avoided (Cheng et al., 2011).

147 The radiative forcing caused by BC has been widely studied. Therefore, in this study, using a  
 148 simplistic model (the following algorithm) the amount of solar radiation absorbed by DOC compared to  
 149 BC was estimated:

$$150 \quad f = \frac{\int_{300}^{2500} I_0(\lambda) \cdot \left\{ 1 - e^{-(\text{MAC}_{365} \left(\frac{365}{\lambda}\right)^{\text{AAE}_{\text{DOC}}} \cdot C_{\text{DOC}} \cdot h_{\text{ABL}})} \right\} d\lambda}{\int_{300}^{2500} I_0(\lambda) \cdot \left\{ 1 - e^{-(\text{MAC}_{550} \left(\frac{550}{\lambda}\right)^{\text{AAE}_{\text{BC}}} \cdot C_{\text{EC}} \cdot h_{\text{ABL}})} \right\} d\lambda} \quad (3)$$



151 where  $\lambda$  is the wavelength;  $I_0(\lambda)$  is the clear sky solar emission spectrum determined using the Air Mass  
152 1 Global Horizontal (AM1GH) irradiance model (Levinson et al., 2010);  $MAC_{365}$  and  $MAC_{550}$  are the  
153 mass absorption cross section of DOC at 365 nm and mass absorption cross section of BC at 550 nm,  
154 respectively;  $h_{ABL}$  is the vertical height of the atmospheric boundary layer; and  $AAE_{DOC}$  and  $AAE_{BC}$  are  
155 the Absorption Ångström Exponents (AAEs) of DOC and BC. In this simplistic model, following a  
156 previous study, we used  $MAC_{550}=7.5 \pm 1.2 \text{ m}^2 \text{ g}^{-1}$  (Bond and Bergstrom, 2006), and AAE for BC was set  
157 as 1, while  $h_{ABL}$  was set to 1000 m, which has little influence on the integration from the wavelengths of  
158 300-2500 nm (Kirillova et al., 2013; Bosch et al., 2014; Kirillova et al., 2014a; Kirillova et al., 2014b).

### 159 2.3.3 In situ DOC bioavailability experiment

160 The bioavailability experiment was conducted from August 17th to 31st, 2015, at the glacier  
161 terminus during fieldwork. In brief, surface ice samples were collected in pre-burned (550 °C, 6 h)  
162 aluminum basins and melted in the field. The melted samples were filtered through pre-burned glass  
163 fiber filters (GF/F 0.7  $\mu\text{m}$ ) into 12 pre-cleaned 125-mL polycarbonate bottles and wrapped with three  
164 layers of aluminum foil to avoid solar irradiation. Two samples were refrigerated immediately after  
165 filtering to obtain initial DOC concentrations; the others were placed outside at the terminus of the glacier,  
166 and 2 samples were refrigerated every 3 days. The BDOC was calculated based on the discrepancies  
167 between initial and treated samples.

## 168 3 Results and discussion

### 169 3.1 DOC concentrations and bioavailability

#### 170 3.1.1 Snowpits

171 LHG glacier is surrounded by arid and semi-arid regions and frequently influenced by strong dust  
172 storms (Dong et al., 2014b) (Fig. 1). Therefore, heavy mineral dust deposition contributes to high DOC  
173 concentrations in LHG glacier. Average DOC concentration of the snowpit samples was  $332.4 \pm 132.3 \mu\text{g}$   
174  $\text{L}^{-1}$  (Fig. 2), with values ranging from  $124.4 \mu\text{g L}^{-1}$  to  $581.0 \mu\text{g L}^{-1}$  (Fig. S1). The highest values appeared  
175 in the dirty layers (Fig. S1), similar to the pattern observed in the Greenland summit snowpit (Hagler et  
176 al., 2007) and glaciers in the southern TP (Xu et al., 2013), indicating DOC concentrations were mainly  
177 influenced by dust deposition in this region. Spatially, our results were higher than those of Tanggula  
178 glacier (TGL) in the middle TP and Rongbuk glacier on Mount Everest (EV) in the southern TP (Fig. 1)  
179 (Table 1) (Yan et al., 2015), which was similar to the distributions of mercury and particle on the TP



180 (Zhang et al., 2012a).

### 181 3.1.2 Surface snow and ice

182 Average DOC concentration in LHG glacier surface snow was significantly lower than that in  
183 surface ice because more impurities were presented in the latter (Fig. 2). Like those of the snowpits, DOC  
184 concentrations in the glacier surface ice (Fig. 2) were higher than those in glacier of the southern TP  
185 (Nyainqentanglha glacier) (Spencer et al., 2014) (Table 1) mainly due to heavy dust load of LHG glacier.  
186 No significant relationship was found between DOC concentration and elevation for either the surface  
187 snow or ice (Fig. S2), suggesting no “altitude effect” of DOC in this glacier. Therefore, the distributions  
188 of DOC concentrations in the glacier surface snow and ice were influenced by complicated factors, such  
189 as the terrain, surface moraine and atmosphere circulation. Furthermore, DOC concentrations of snow  
190 and ice of this glacier were within the range of previously reported values for glaciated regions outside  
191 the TP (Table 1).

### 192 3.1.3 DOC bioavailability

193 Previous studies conducted under controlled conditions (stable temperature) have shown that  
194 glacier-derived DOC was more bioavailable than those of terrestrial-derived DOC (Hood et al., 2009;  
195 Fellman et al., 2010). Our results showed that the amount of DOC being consumed decreased  
196 exponentially over time ( $R^2=0.98$ ) (Fig. 3), with approximately 26.7% (from  $416.9 \mu\text{g L}^{-1}$  to  $305.6 \mu\text{g L}^{-1}$ )  
197 degraded within 15 days during the experiment (average temperature:  $3.8 \pm 3.7 \text{ }^\circ\text{C}$ ; range:  $-4.8$ - $11.4 \text{ }^\circ\text{C}$ ).  
198 BDOC reached 43.2% if the experiment duration was extended to 28 days, according to the equation  
199 derived from the 15-day experiment (Fig. 3). Despite different incubation conditions, this finding agreed  
200 well with the reports of BDOC from a glacier in the southern TP (28-day dark incubation at  $20 \text{ }^\circ\text{C}$ , 46-  
201 69% BDOC) (Spencer et al., 2014) and European Alpine glaciers (50-day dark incubation at  $4 \text{ }^\circ\text{C}$ ,  
202  $59 \pm 20\%$  BDOC) (Singer et al., 2012). Therefore, the previous results obtained in the laboratory are close  
203 to the reality and can be used to estimate the bioavailability of glacier-derived DOC.

### 204 3.2 Sources of snowpit DOC

205 The sources of glacier DOC are diverse and include microbial activities (viruses, bacteria and algae)  
206 (Anesio et al., 2009), terrestrial inputs (DOC deposition from vascular plants and dust) (Singer et al.,  
207 2012) and anthropogenic sources (fossil fuel and biomass combustion) (Stubbins et al., 2012). In this  
208 study, major ions were adopted as indicators to investigate the potential sources of snowpit DOC, because





209 the sources of major ions in snowpit samples from Tibetan glaciers have been investigated in detail (Kang  
210 et al., 2002; Kang et al., 2008). It was found that DOC and  $\text{Ca}^{2+}$  (a typical indicator of mineral dust) were  
211 significantly related ( $R^2=0.84$ , Fig. S3), suggesting that the major source of DOC was mineral dust, which  
212 is consistent with the previous DOC source investigations of snowpits on this glacier (Yan et al., 2015).  
213 In addition, the combined study of geochemistry and backward trajectories for LHG glacier showed that  
214 the dust particles on the glacier were mainly derived from the deserts to the west and north of the study  
215 area (Dong et al., 2014a).

### 216 3.3 Light absorption characteristics of DOC

#### 217 3.3.1 AAE

218 AAE is generally used to characterize the spectral dependence of the light absorption of DOC, which  
219 is important input data for radiative forcing calculations. The fitted  $\text{AAE}_{330-400}$  values ranged from 1.2 to  
220 15.2 ( $5.0 \pm 5.9$ ) for snow samples and from 0.3 to 8.4 ( $3.4 \pm 2.7$ ) for ice samples (Fig. S5). The relatively  
221 low  $\text{AAE}_{330-400}$  values of ice indicated that the DOC experienced strong photo-bleaching due to long-  
222 duration exposure to solar irradiation. Previous studies have found that the AAE of brown carbon (BrC)  
223 in aged aerosols (Zhao et al., 2015) and secondary organic aerosols (SOAs) (Lambe et al., 2013) were  
224 much lower compared to that of the primary values. Therefore, the large divergence in AAE values might  
225 suggest different chemical compositions of DOC due to multiple possibilities, such as different sources  
226 and photo-bleaching processes. In general,  $\text{AAE}_{330-400}$  had a negative relationship with  $\text{MAC}_{365}$ ,  
227 especially in the ice samples (Fig. S5), suggesting that stronger absorbing DOC might contribute to lower  
228 AAE values, which was also found in other aerosol studies (Chen and Bond, 2010; Bosch et al., 2014;  
229 Kirillova et al., 2014b).

#### 230 3.3.2 $\text{MAC}_{365}$

231  $\text{MAC}_{365}$  for DOC is another input data point for the radiative forcing calculation. The light  
232 absorption ability at 365 nm is selected to avoid interferences of non-organic compounds (such as nitrate)  
233 and to be consistent with previous investigations (Hecobian et al., 2010; Cheng et al., 2011). The  $\text{MAC}_{365}$   
234 of DOC was  $1.4 \pm 0.4 \text{ m}^2 \text{ g}^{-1}$  in snow and  $1.3 \pm 0.7 \text{ m}^2 \text{ g}^{-1}$  in glacier ice (Fig. S5). The MAC values for  
235 DOC from different sources varied widely. Normally, the  $\text{MAC}_{365}$  of DOC derived from biomass  
236 combustion was as high as  $5 \text{ m}^2 \text{ g}^{-1}$  (Kirchstetter, 2004). Correspondingly, the value for SOAs was as  
237 low as  $0.001\text{-}0.088 \text{ m}^2 \text{ g}^{-1}$  (Lambe et al., 2013) and humic like substances (HULIS) in Arctic snow was  
238  $2.6 \pm 1.1$  at 250 nm (Voisin et al., 2012) (Table 2). Due to the remote location of LHG glacier, it was



239 considered that the snowpit DOC should be SOAs with low  $MAC_{365}$  values, however, the high  $MAC_{365}$   
240 value of the snowpit DOC indicated that these DOC may not be entirely derived from SOAs. Therefore,  
241 it was proposed that mineral dust-sourced DOC caused high  $MAC_{365}$  values in the snowpit samples. The  
242 light absorption characteristics of DOC from both snowpit and ice showed similar patterns to those of  
243 WSOC in dust from the adjacent deserts, further indicating that LHG glacier DOC was transported via  
244 mineral dust and shared similar light absorption characteristics (Fig. 4). Moreover, the difference in light  
245 absorption characteristics (especially for wavelengths larger than 400 nm) between snow/ice samples  
246 and aerosols in Beijing, China, also indicated different sources (Fig. 4) (Table 2). Light absorbance was  
247 significantly correlated with DOC concentrations in both snow and ice samples (Fig. S4), suggesting that  
248 DOC was one of the absorption factors. Nevertheless,  $MAC_{365}$  values of surface ice (0-3 cm) were lower  
249 than those of subsurface layers (3-5 cm), despite its higher DOC concentrations (Fig. 5), reflecting  
250 stronger DOC photo-bleaching in the surface ice due to the direct exposure to solar irradiation.

### 251 3.3.3 Radiative forcing of DOC relative to BC

252 The radiative forcing contributed by WSOC relative to BC in aerosols has been proposed to be as  
253 high as 2-10 % (Kirillova et al., 2013; Kirillova et al., 2014a). Furthermore, it was estimated that BrC  
254 accounted for a higher ratio of 20 % of the direct radiative forcing of aerosols at the top of the atmosphere  
255 because BC concentrations decrease faster than BrC in the high-altitude atmosphere (Liu et al., 2014).  
256 Because the studied glacier is located at high elevations near the top of the troposphere and features  
257 relatively high DOC/BC ratios in the snowpit samples (Fig. S6), the radiative forcing caused by DOC  
258 relative to BC should also be high.

259 Our results showed that the relative radiative forcing caused by DOC relative to BC ranged from  
260 2.1 % to 30.4 % ( $9.5 \pm 8.4$  %) for snowpit samples and from 0.01% to 0.5 % ( $0.1 \pm 0.1$  %) for surface ice  
261 samples (Fig. S5), mainly because of the higher DOC/BC ratio (0.65) in the snowpit samples than in the  
262 ice samples (0.012) (Fig. S6). The value in ice was much lower due to the enrichment of BC in surface  
263 glacier ice during the intensive ablation period (Xu et al., 2009). Because snowpit samples can be  
264 approximately considered to be fresh snow; thus, radiative forcing caused by DOC is a non-ignorable  
265 contributor in addition to BC in reducing the albedo of a glacier when the glacier is covered by fresh  
266 snow.

### 267 3.4 DOC export during the melt season

268 The two-year average discharge-weighted DOC concentration was  $237.5 \pm 95.6 \mu\text{g L}^{-1}$  during the



269 melting period, comparable with the proglacial streamwater of Mount Nyainqentanglha glacier in the  
270 southern TP (Spencer et al., 2014). Seasonally, high DOC concentrations appeared during the low  
271 discharge periods (May to July and September to October) (Fig. 6), suggesting that DOC concentrations  
272 were slightly enriched to some extent. However, there were no clear diurnal variations in DOC  
273 concentrations with the discharge, indicating that the discharge from different parts of the glacier was  
274 well mixed at the glacier terminus (Fig. S7).

275 The seasonal variations in DOC flux were similar to those of the discharge (Fig. 6), indicating that  
276 discharge (rather than DOC concentrations) played a dominant role in the DOC mass flux. Hence, the  
277 majority of the glacier DOC export occurred during the summer melting season. Over the whole melting  
278 season, the annual flux of DOC from LHG glacier was  $340.7 \text{ kg km}^{-2} \text{ yr}^{-1}$ , with peak DOC fluxes from  
279 mid-late July to late August (70% of annual flux). Combined with the value of BDOC determined above,  
280 at least  $3,001.5 \text{ kg C yr}^{-1}$  was ready to be decomposed and returned to the atmosphere as  $\text{CO}_2$  within 28  
281 days of its release, producing a positive feedback in the global warming process.

#### 282 **4 Conclusions and implications**

283 The concentrations and light absorption characteristics of DOC on a typical glacier in the northern  
284 TP were reported in this study. The mean DOC concentrations in snowpit sample, fresh snow, surface ice  
285 and proglacial streamwater were  $332.4 \pm 132.3 \mu\text{g L}^{-1}$ ,  $229.3 \pm 104.4 \mu\text{g L}^{-1}$ ,  $425.8 \pm 269.9 \mu\text{g L}^{-1}$  and  
286  $237.5 \pm 95.6 \mu\text{g L}^{-1}$ , respectively. These values were slightly higher or comparable to those of other regions,  
287 such as the European Alps and Alaska. DOC in snowpit samples was significantly correlated with  $\text{Ca}^{2+}$ ,  
288 a typical cation in mineral dust, indicating that mineral dust transported from adjacent arid regions made  
289 important contributions to DOC of the studied glacierized region. In addition, the light absorption profile  
290 of snowpit DOC was similar to that of dust from potential source deserts, providing further evidence of  
291 the influence of mineral dust on snowpit DOC. For the first time, it is estimated that the radiative forcing  
292 caused by DOC accounted for  $9.5 \pm 8.4 \%$  and  $0.1 \pm 0.1 \%$  relative to that of BC, in the snowpit samples  
293 and surface ice, respectively. Therefore, in addition to BC, DOC is also an important agent in terms of  
294 absorbing solar irradiation in the glacierized region, especially when the glacier is covered by fresh snow,  
295 which contains high DOC/BC ratios. It has also been proven that water-insoluble organic carbon has a  
296 stronger light absorption ability (Chen and Bond, 2010). Therefore, the total contribution of OC to light  
297 absorption in the glacierized region should be higher, which requires further study. Wet deposition is the  
298 most effective way of removing carbonaceous matter from the atmosphere (Vignati et al., 2010), and the



299 removal ratio of OC in remote areas is almost the same as that of BC after long-range transport from  
300 source regions (Garrett et al., 2011). Because snowpit samples directly reflect the wet and dry depositions  
301 of carbonaceous matter, it is assumed that the contribution of radiative forcing for WSOC relative to BC  
302 in the atmosphere in glacierized regions should be close to that of the snowpit samples in this study.

303 Because proglacial streamwater from different parts of the glacier is well mixed, no clear diurnal  
304 variations in DOC concentrations have been found. Combined with discharge and the corresponding  
305 DOC concentration, it was calculated that approximately  $340.7 \text{ kg km}^{-2} \text{ yr}^{-1}$  of DOC was released from  
306 LHG glacier. It was also calculated that approximately 43.2% of the DOC could be decomposed within  
307 28 days; thus,  $3,001.5 \text{ kg C yr}^{-1}$  would return to the atmosphere as  $\text{CO}_2$ , producing positive feedback in  
308 the warming process. Although the flux of DOC from the studied glacier is small, the number of glacial  
309 rivers across the entire TP and surrounding areas may be large due to the glacial area of approximately  
310  $100,000 \text{ km}^2$  (Yao et al. 2012). These factors need to be comprehensively studied in the future.

311

312

313 *Author contributions.* S. Kang was the lead scientist of the entire project. F. Yan wrote the first draft of the manuscript  
314 with the significant help of C. Li. F. Yan did DOC and ions measurement. Y. Li and Y. Zhang helped with the sample  
315 collection. X. Qin and X. Zhang provided the discharge data. M. Sillanpää, B. Qu, P. Chen, Z. Hu and X. Li improved  
316 the manuscript. S. Kang and C. Li conceived and designed the experiments.

317

318 *Acknowledgements.* This study was supported by the National Nature Science Foundation of China (41225002,  
319 41271015, 41121001), State Key Laboratory of Cryospheric Science (SKLCS-ZZ-2015-10 and SKLCS-OP-2014-  
320 05) and the Academy of Finland (decision number 268170). The authors acknowledge the staff of the Qilian Shan  
321 Station of Glaciology and Ecological Environment, Chinese Academy of Science.

322

323

#### 324 **References**

- 325 Andreae, M. and Gelencsér, A.: Black carbon or brown carbon? The nature of light-absorbing carbonaceous aerosols,  
326 *Atmospheric Chemistry and Physics*, 6, 3131-3148, 2006.
- 327 Anesio, A. M., Hodson, A. J., Fritz, A., Psenner, R., and Sattler, B.: High microbial activity on glaciers: importance  
328 to the global carbon cycle, *Global Change Biology*, 15, 955-960, 2009.
- 329 Anesio, A. M. and Laybourn-Parry, J.: Glaciers and ice sheets as a biome, *Trends in Ecology & Evolution*, 27, 219-



- 330 225, 2012.
- 331 Antony, R., Mahalinganathan, K., Thamban, M., and Nair, S.: Organic Carbon in Antarctic Snow: Spatial Trends  
332 and Possible Sources, *Environmental Science & Technology*, 45, 9944-9950, 2011.
- 333 Bhatia, M. P., Das, S. B., Longnecker, K., Charette, M. A., and Kujawinski, E. B.: Molecular characterization of  
334 dissolved organic matter associated with the Greenland ice sheet, *Geochimica et Cosmochimica Acta*, 74, 3768-  
335 3784, 2010.
- 336 Bhatia, M. P., Das, S. B., Xu, L., Charette, M. A., Wadham, J. L., and Kujawinski, E. B.: Organic carbon export from  
337 the Greenland ice sheet, *Geochimica et Cosmochimica Acta*, 109, 329-344, 2013.
- 338 Bond, T. C., and Bergstrom, R. W.: Light Absorption by Carbonaceous Particles: An Investigative Review, *Aerosol  
339 Science and Technology*, 40, 27-67, 10.1080/02786820500421521, 2006.
- 340 Bosch, C., Andersson, A., Kirillova, E. N., Budhavant, K., Tiwari, S., Praveen, P., Russell, L. M., Beres, N. D.,  
341 Ramanathan, V., and Gustafsson, Ö.: Source - diagnostic dual - isotope composition and optical properties of  
342 water - soluble organic carbon and elemental carbon in the South Asian outflow intercepted over the Indian Ocean,  
343 *Journal of Geophysical Research: Atmospheres*, 119, 11,743-711,759, 2014.
- 344 Chen, Y. and Bond, T. C.: Light absorption by organic carbon from wood combustion, *Atmospheric Chemistry and  
345 Physics*, 10, 1773-1787, 2010.
- 346 Cheng, Y., He, K. B., Zheng, M., Duan, F. K., Du, Z. Y., Ma, Y. L., Tan, J. H., Yang, F. M., Liu, J. M., Zhang, X. L.,  
347 Weber, R. J., Bergin, M. H., and Russell, A. G.: Mass absorption efficiency of elemental carbon and water-soluble  
348 organic carbon in Beijing, China, *Atmospheric Chemistry and Physics*, 11, 11497-11510, 2011.
- 349 Dong, Z., Qin, D., Chen, J., Qin, X., Ren, J., Cui, X., Du, Z., and Kang, S.: Physicochemical impacts of dust particles  
350 on alpine glacier meltwater at the Laohugou Glacier basin in western Qilian Mountains, China, *The Science of  
351 the total environment*, 493, 930-942, 2014a.
- 352 Dong, Z., Qin, D., Kang, S., Ren, J., Chen, J., Cui, X., Du, Z., and Qin, x.: Physicochemical characteristics and  
353 sources of atmospheric dust deposition in snow packs on the glaciers of western Qilian Mountains, China, *Tellus  
354 B*, 66, 2014b.
- 355 Du, W., Qin, X., Liu, Y. S., and Wang, X. F.: Variation of Laohugou Glacier No. 12 in Qilian Mountains *Journal of  
356 Glaciology and Geocryology*, 30, 373-379, 2008.
- 357 Fellman, J. B., Hood, E., Raymond, P. A., Stubbins, A., and Spencer, R. G. M.: Spatial Variation in the Origin of  
358 Dissolved Organic Carbon in Snow on the Juneau Icefield, Southeast Alaska, *Environmental Science &  
359 Technology*, doi: 10.1021/acs.est.5b02685, 2015. 2015.
- 360 Fellman, J. B., Spencer, R. G. M., Hernes, P. J., Edwards, R. T., D'Amore, D. V., and Hood, E.: The impact of glacier  
361 runoff on the biodegradability and biochemical composition of terrigenous dissolved organic matter in near-shore  
362 marine ecosystems, *Marine Chemistry*, 121, 112-122, 2010.
- 363 Fitzgerald, W. F.: Clean hands, dirty hands: Clair Patterson and the aquatic biogeochemistry of mercury, *Clean Hands:  
364 Clair Patterson's Crusade Against Environmental Lead Contamination*, 1999. 119-137, 1999.
- 365 Garrett, T. J., Brattström, S., Sharma, S., Worthy, D. E. J., and Novelli, P.: The role of scavenging in the seasonal  
366 transport of black carbon and sulfate to the Arctic, *Geophysical Research Letters*, 38, n/a-n/a, 2011.
- 367 Hagler, G. S. W., Bergin, M. H., Smith, E. A., Dibb, J. E., Anderson, C., and Steig, E. J.: Particulate and water-  
368 soluble carbon measured in recent snow at Summit, Greenland, *Geophysical Research Letters*, 34, n/a-n/a, 2007.
- 369 Hecobian, A., Zhang, X., Zheng, M., Frank, N., Edgerton, E. S., and Weber, R. J.: Water-Soluble Organic Aerosol  
370 material and the light-absorption characteristics of aqueous extracts measured over the Southeastern United States,  
371 *Atmospheric Chemistry and Physics*, 10, 5965-5977, 2010.
- 372 Hood, E., Battin, T. J., Fellman, J., O'Neel, S., and Spencer, R. G. M.: Storage and release of organic carbon from  
373 glaciers and ice sheets, *Nature Geoscience*, 8, 91-96, 2015.



- 374 Hood, E., Fellman, J., Spencer, R. G., Hernes, P. J., Edwards, R., D'Amore, D., and Scott, D.: Glaciers as a source  
375 of ancient and labile organic matter to the marine environment, *Nature*, 462, 1044-1047, 2009.
- 376 Jacob, T., Wahr, J., Pfeffer, W. T., and Swenson, S.: Recent contributions of glaciers and ice caps to sea level rise,  
377 *Nature*, 482, 514-518, 2012.
- 378 Kang, S., Mayewski, P. A., Qin, D., Yan, Y., Hou, S., Zhang, D., Ren, J., and Kruetz, K.: Glaciochemical records  
379 from a Mt. Everest ice core: relationship to atmospheric circulation over Asia, *Atmospheric Environment*, 36,  
380 3351-3361, 2002.
- 381 Kang, S., Wang, F., Morgenstern, U., Zhang, Y., Grigholm, B., Kaspari, S., Schwikowski, M., Ren, J., Yao, T., Qin,  
382 D., and Mayewski, P. A.: Dramatic loss of glacier accumulation area on the Tibetan Plateau revealed by ice core  
383 tritium and mercury records, *The Cryosphere*, 9, 1213-1222, 2015.
- 384 Kang, S., Xu, Y., You, Q., Flügel, W.-A., Pepin, N., and Yao, T.: Review of climate and cryospheric change in the  
385 Tibetan Plateau, *Environmental Research Letters*, 5, 015101, 2010.
- 386 Kang, S. C., Huang, J., and Xu, Y. W.: Changes in ionic concentrations and  $\delta^{18}O$  in the snowpack of Zhadang glacier,  
387 Nyainqentanglha mountain, southern Tibetan Plateau, *Annals of Glaciology*, 49, 127-134, 2008.
- 388 Kaspari, S., Painter, T. H., Gysel, M., Skiles, S. M., and Schwikowski, M.: Seasonal and elevational variations of  
389 black carbon and dust in snow and ice in the Solu-Khumbu, Nepal and estimated radiative forcings, *Atmospheric  
390 Chemistry and Physics*, 14, 8089-8103, 2014.
- 391 Kirchstetter, T. W.: Evidence that the spectral dependence of light absorption by aerosols is affected by organic  
392 carbon, *Journal of Geophysical Research*, 109, 2004.
- 393 Kirillova, E. N., Andersson, A., Han, J., Lee, M., and Gustafsson, Ö.: Sources and light absorption of water-soluble  
394 brown carbon aerosols in the outflow from northern China, *Atmospheric Chemistry and Physics Discussions*, 13,  
395 19625-19648, 2013.
- 396 Kirillova, E. N., Andersson, A., Han, J., Lee, M., and Gustafsson, Ö.: Sources and light absorption of water-soluble  
397 organic carbon aerosols in the outflow from northern China, *Atmospheric Chemistry and Physics*, 14, 1413-1422,  
398 2014a.
- 399 Kirillova, E. N., Andersson, A., Tiwari, S., Srivastava, A. K., Bisht, D. S., and Gustafsson, Ö.: Water-soluble organic  
400 carbon aerosols during a full New Delhi winter: Isotope-based source apportionment and optical properties,  
401 *Journal of Geophysical Research: Atmospheres*, 119, 3476-3485, 2014b.
- 402 Lambe, A. T., Cappa, C. D., Massoli, P., Onasch, T. B., Forestieri, S. D., Martin, A. T., Cummings, M. J., Croasdale,  
403 D. R., Brune, W. H., and Worsnop, D. R.: Relationship between oxidation level and optical properties of secondary  
404 organic aerosol, *Environmental science & technology*, 47, 6349-6357, 2013.
- 405 Lawson, E. C., Wadham, J. L., Tranter, M., Stibal, M., Lis, G. P., Butler, C. E. H., Laybourn-Parry, J., Nienow, P.,  
406 Chandler, D., and Dewsbury, P.: Greenland Ice Sheet exports labile organic carbon to the Arctic oceans,  
407 *Biogeosciences*, 11, 4015-4028, 2014.
- 408 Legrand, M., Preunkert, S., Jourdain, B., Guilhermet, J., Fain, X., Alekhina, I., and Petit, J. R.: Water-soluble organic  
409 carbon in snow and ice deposited at Alpine, Greenland, and Antarctic sites: a critical review of available data and  
410 their atmospheric relevance, *Climate of the Past Discussions*, 9, 2357-2399, 2013.
- 411 Levinson, R., Akbari, H., and Berdahl, P.: Measuring solar reflectance—Part I: Defining a metric that accurately  
412 predicts solar heat gain, *Solar Energy*, 84, 1717-1744, 2010.
- 413 Li, C., Kang, S., Zhang, Q., and Kaspari, S.: Major ionic composition of precipitation in the Nam Co region, Central  
414 Tibetan Plateau, *Atmospheric Research*, 85, 351-360, 2007.
- 415 Li, J., Qin, X., Sun, W., Zhang, M., and Yang, J.: Analysis on Micrometeorological Characteristic in the Surface Layer  
416 of Laohugou Glacier No.12 Qilian Mountains, *Plateau Meteorology*, 31, 370-379, 2012.
- 417 Li, Z., Li, H., Dong, Z., and Zhang, M.: Chemical characteristics and environmental significance of fresh snow



- 418 deposition on Urumqi Glacier No. 1 of Tianshan Mountains, China, *Chinese Geographical Science*, 20, 389-397,  
419 2010.
- 420 Liu, J., Scheuer, E., Dibb, J., Ziemba, L. D., Thornhill, K., Anderson, B. E., Wisthaler, A., Mikoviny, T., Devi, J. J.,  
421 and Bergin, M.: Brown carbon in the continental troposphere, *Geophysical Research Letters*, 41, 2191-2195, 2014.
- 422 May, B., Wagenbach, D., Hoffmann, H., Legrand, M., Preunkert, S., and Steier, P.: Constraints on the major sources  
423 of dissolved organic carbon in Alpine ice cores from radiocarbon analysis over the bomb - peak period, *Journal*  
424 *of Geophysical Research: Atmospheres*, 118, 3319-3327, 2013.
- 425 Qu, B., Ming, J., Kang, S. C., Zhang, G. S., Li, Y. W., Li, C. D., Zhao, S. Y., Ji, Z. M., and Cao, J. J.: The decreasing  
426 albedo of the Zhadang glacier on western Nyainqentanglha and the role of light-absorbing impurities, *Atmospheric*  
427 *Chemistry and Physics*, 14, 11117-11128, 2014.
- 428 Rignot, E., Rivera, A., and Casassa, G.: Contribution of the Patagonia Icefields of South America to sea level rise,  
429 *Science*, 302, 434-437, 2003.
- 430 Singer, G. A., Fasching, C., Wilhelm, L., Niggemann, J., Steier, P., Dittmar, T., and Battin, T. J.: Biogeochemically  
431 diverse organic matter in Alpine glaciers and its downstream fate, *Nature Geoscience*, 5, 710-714, 2012.
- 432 Spencer, R. G. M., Guo, W., Raymond, P. A., Dittmar, T., Hood, E., Fellman, J., and Stubbins, A.: Source and  
433 biolability of ancient dissolved organic matter in glacier and lake ecosystems on the Tibetan Plateau, *Geochimica*  
434 *et Cosmochimica Acta*, 142, 64-74, 2014.
- 435 Stubbins, A., Hood, E., Raymond, P. A., Aiken, G. R., Sleighter, R. L., Hernes, P. J., Butman, D., Hatcher, P. G.,  
436 Striegl, R. G., Schuster, P., Abdulla, H. A. N., Vermilyea, A. W., Scott, D. T., and Spencer, R. G. M.:  
437 Anthropogenic aerosols as a source of ancient dissolved organic matter in glaciers, *Nature Geoscience*, 5, 198-  
438 201, 2012.
- 439 Vignati, E., Karl, M., Krol, M., Wilson, J., Stier, P., and Cavalli, F.: Sources of uncertainties in modelling black  
440 carbon at the global scale, *Atmospheric chemistry and physics*, 10, 2595-2611, 2010.
- 441 Voisin, D., Jaffrezo, J. L., Houdier, S., et al. Carbonaceous species and humic like substances (HULIS) in Arctic  
442 snowpack during OASIS field campaign in Barrow[J]. *Journal of Geophysical Research: Atmospheres*, 2012,  
443 117(D14).
- 444 Xu, B., Cao, J., Hansen, J., Yao, T., Joswia, D. R., Wang, N., Wu, G., Wang, M., Zhao, H., and Yang, W.: Black soot  
445 and the survival of Tibetan glaciers, *Proceedings of the National Academy of Sciences*, 106, 22114-22118, 2009.
- 446 Xu, J., Zhang, Q., Li, X., Ge, X., Xiao, C., Ren, J., and Qin, D.: Dissolved organic matter and inorganic ions in a  
447 central Himalayan glacier--insights into chemical composition and atmospheric sources, *Environ Sci Technol*, 47,  
448 6181-6188, 2013.
- 449 Yan, F., Kang, S., Chen, P., LI, Y., Hu, Z., and Li, C.: Concentration and Source of dissolved organic carbon in  
450 snowpits of the Tibetan Plateau, *Environmental Science*, 8, 2827-2832, 2015.
- 451 Yao, T., Thompson, L., Yang, W., Yu, W., Gao, Y., Guo, X., Yang, X., Duan, K., Zhao, H., Xu, B., Pu, J., Lu, A.,  
452 Xiang, Y., Kattel, D. B., and Joswiak, D.: Different glacier status with atmospheric circulations in Tibetan Plateau  
453 and surroundings, *Nature Climate Change*, doi: 10.1038/nclimate1580, 2012. 2012.
- 454 Zhang, Q., Huang, J., Wang, F., Mark, L., Xu, J., Armstrong, D., Li, C., Zhang, Y., and Kang, S.: Mercury distribution  
455 and deposition in glacier snow over western China, *Environmental science & technology*, 46, 5404-5413, 2012a.
- 456 Zhang, Y., Liu, S., Shangguan, D., Li, J., and Zhao, J.: Thinning and shrinkage of Laohugou No. 12 glacier in the  
457 Western Qilian Mountains, China, from 1957 to 2007, *Journal of Mountain Science*, 9, 343-350, 2012b.
- 458 Zhao, R., Lee, A. K. Y., Huang, L., Li, X., Yang, F., and Abbatt, J. P. D.: Photochemical processing of aqueous  
459 atmospheric brown carbon, *Atmospheric Chemistry and Physics Discussions*, 15, 2957-2996, 2015.
- 460



461 **Table 1.** Comparison of DOC concentrations in snow and ice from the glacier in this study and other regions.

Sites	DOC concentration ( $\mu\text{g L}^{-1}$ )	Sample types	References
Laohugou glacier (LHG)	332.4 $\pm$ 132.3	Snowpit	This study
Tanggula glacier (TGL)	216.9 $\pm$ 142.8	Snowpit	(Yan et al., 2015)
Mount Everest (EV)	152.5 $\pm$ 56.1	Snowpit	
Mendenhall Glacier, Alaska	190	snowpit	(Stubbins et al., 2012)
Greenland ice sheet	40.3-56.9	Snowpit	(Hagler et al., 2007)
Laohugou glacier (LHG)	229.3 $\pm$ 104.4	Surface snow	This study
Greenland ice sheet	111.2	Surface snow	(Hagler et al., 2007)
Juneau Icefield, Southeast Alaska	100-300	Fresh snow/snowpits	(Fellman et al., 2015)
Laohugou glacier (LHG)	425.8 $\pm$ 269.9	Surface ice	This study
Mount Nyainqentanglha Glacier	212.4	Glacier ice	(Spencer et al., 2014)
Antarctic ice sheet	460 $\pm$ 120	Surface ice	(Hood et al., 2015)
Alpine glacier	138 $\pm$ 96	Subsurface ice	(Singer et al., 2012)
Laohugou glacier (LHG)	237.5 $\pm$ 95.6	Proglacial streamwater	This study
Mount Nyainqentanglha Glacier	261.6	Proglacial streamwater	(Spencer et al., 2014)
Mendenhall Glacier, Alaska	380 $\pm$ 20	Proglacial streamwater	(Stubbins et al., 2012)

462

463





464 **Table 2.** Mass absorption cross section (MAC) and Absorption Ångström Exponent (AAE<sub>330-400</sub>) of ice and snow  
 465 from LHG glacier and aerosols from other regions.

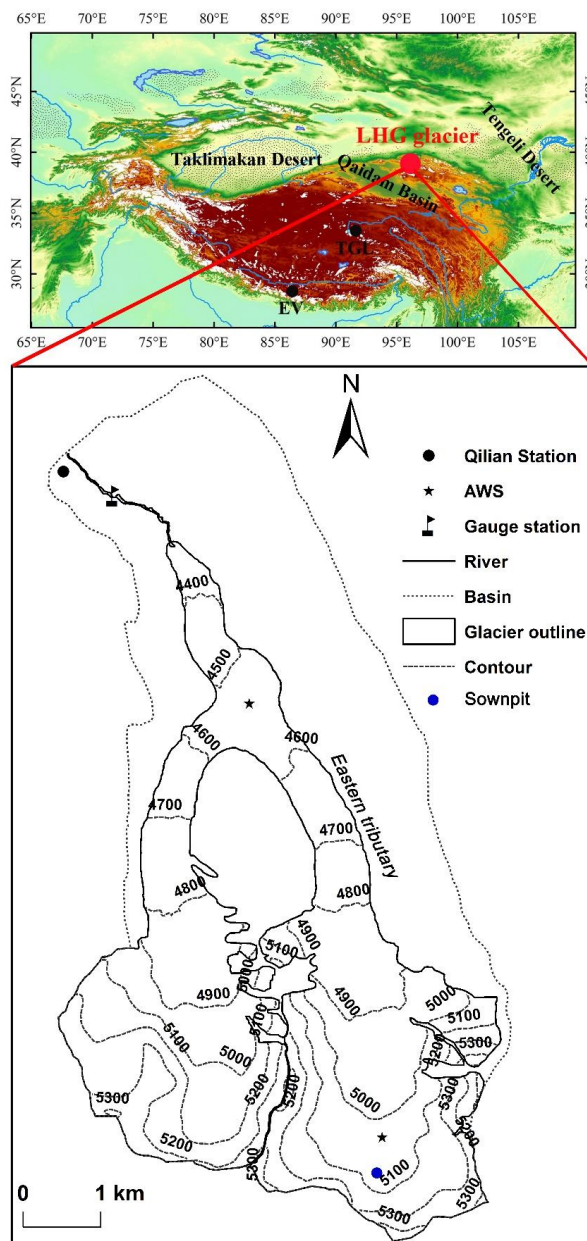
Site/Source	MAC (m <sup>2</sup> g <sup>-1</sup> )	AAE	λ	References
LHG glacier	1.4±0.4 (snow)	5.0±5.9 (snow)	365	This study
	1.3±0.7 (ice)	3.4±2.7 (ice)		
Biomass smoke	5.0	4.8	350	(Kirchstetter, 2004)
Secondary organic aerosols	0.001-0.088	5.2-8.8	405	(Lambe et al., 2013)
Wood smoke	0.13-1.1	8.6-17.8	400	(Chen and Bond, 2010)
HULIS, Arctic snow	2.6±1.1	6.1 <sup>a</sup>	250	(Voisin et al., 2012)
Beijing, China (winter)	1.79±0.24	7.5	365	(Cheng et al., 2011)
Beijing, China (summer)	0.71±0.20	7.1	365	(Cheng et al., 2011)

466 <sup>a</sup> AAE 的波长范围为 300-550 nm

467

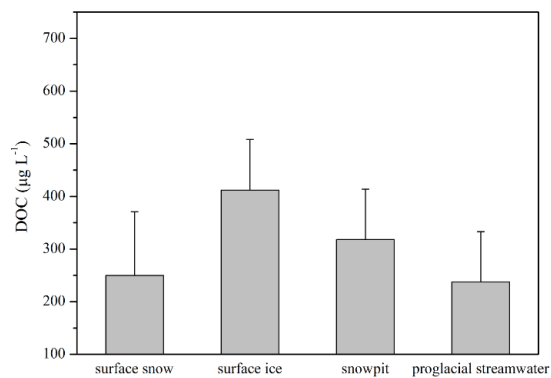


468 Figure 1. Location map of LHG glacier No. 12.  
469 Figure 2. Average DOC concentrations of ice, snow and proglacial streamwater of LHG glacier.  
470 Figure 3. Exponential decreases in DOC concentrations during the biodegradation experiment. Note: The blue point  
471 is calculated using equations derived from the experimental data (black point).  
472 Figure 4. Absorption spectra for DOC in snow and ice of LHG glacier and the dust and desert sand from surrounding  
473 areas.  
474 Figure 5. Comparison of DOC concentrations (A) and  $MAC_{365}$  (B) between surface and subsurface ice.  
475 Figure 6. The discharge, DOC concentrations and fluxes exported from LHG glacier. Note: The concentrations with  
476 error bars include more than one sample on that day.  
477  
478



479  
480  
481  
482  
483

Figure 1. Location map of Laohugou glacier No. 12.

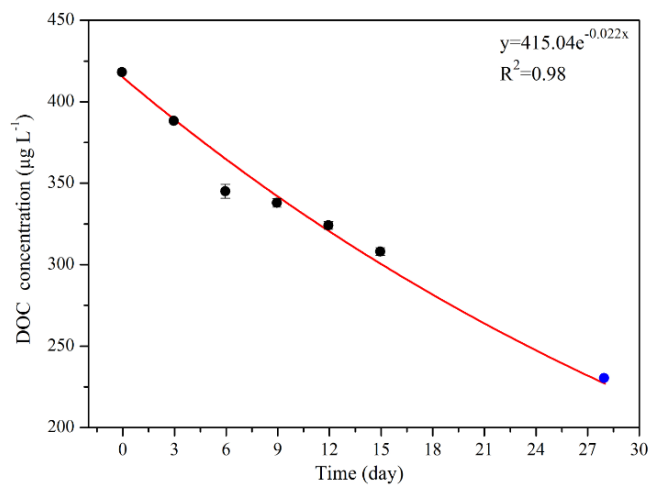


484

485

**Figure 2.** Average DOC concentrations of ice, snow and proglacial streamwater of LHG glacier.

486



487

488

**Figure 3.** Exponential decreases in DOC concentrations during the biodegradation experiment. Note: The blue

489

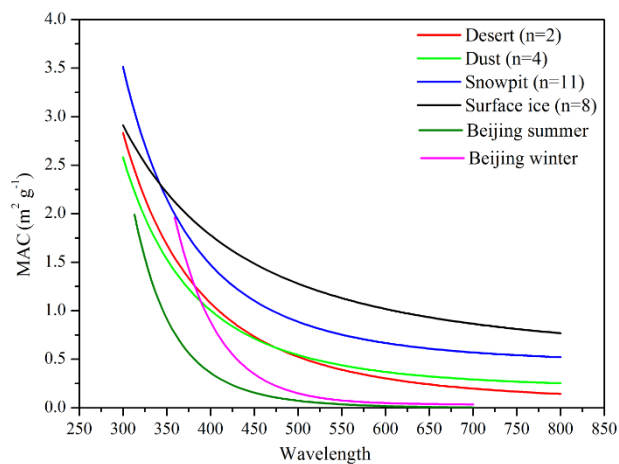
point is calculated using equations derived from the experimental data (black point). Mean values  $\pm$  standard

490

deviation of duplicate treated samples are presented.

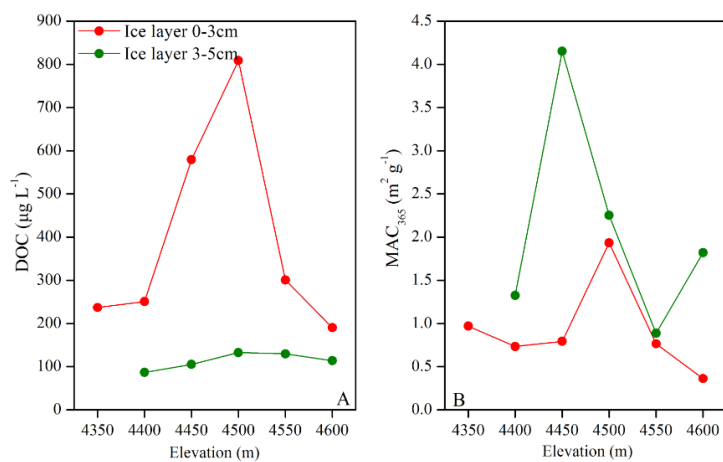
491

492



493  
494  
495  
496  
497  
498

**Figure 4.** Absorption spectra for DOC in snow and ice of LHG glacier and the dust and desert sand from surrounding areas.



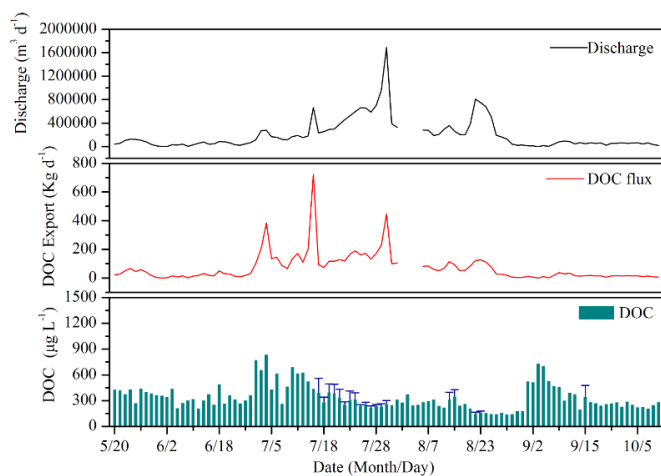
499

500

**Figure 5.** Comparison of DOC concentrations (A) and  $\text{MAC}_{365}$  (B) between surface and subsurface ice.

501

502



503

504

505

**Figure 6.** The discharge, DOC concentrations and fluxes exported from LHG glacier. Note: The concentrations with error bars include more than one sample on that day.

506

507